Revista Brasileira de Física, Vol. 9, NP 1, 1979

Astronomical Observations with the Optical Multichannel Analyser of the São Paulo University

S. J. CODINA-LANDABERRY and J. A. de FREITAS PACHECO

Instituto Astronômico e Geofísico, universidade de São Paulo, SP

Recebido eni 13 de Janeiro de **1978**

We report the first astronomical observations made with the optical multichannel analyser (OMA) of the São Paulo University. A detailed description of the instrumentation is given as well as the results derived from the observation of some emission nebulae.

Apresentamos as primeiras observações astronômicas realizadas com o sistema multicanal óptico da Universidade de São Paulo. Uma descrição detalhada do instrumental é dada, bem como os resultados obtidos das observações de algumas nebulosas em emissão.

1. INTRODUCTION

The field of light detection techniques for astronomical purposes has been enormously developed in these last few years. New solid-state detectors have allowed the improvement of the recording of stellar spectra through optical multi-channels as well as the data analysis, since these sensors provide a linear out-put with respect the light intensity. Besides that, these detectors present other advantages as compared to a photographic plate: higher quantum efficiency a larger spectral response.

In this work we describe in detail the new astronomical optical multi-channel attached recently to the 61 cm telescope of the Abrahão de Moraes Observatory at Valinhos. We report also the first observations of diffuse nebulae made with this instrumentation. Two pla-

netary nebulae (NGC 6818 and NGC 7009) and two H II regions (Orion and "Lagoon" nebulae) were observed.

In section 2, we describe the optical systern (telescope and spectrograph) and the detector systern (silicon-vidicon) used in these observations. In the following sections we present our observations and the results obtained. We compare our data and the physical parameters deduced for these diffuse nebulae with previous observations in order to have a reference for the perforrnance of the equipment.

2. INSTRUMENTATION

The equiprnent used is a reflector telescope coupled to a matched standard grating spectrograph which feeds an optical rnultichannel analyzer, according to the following description.

Telescope

The telescope is a standard Boller & Chivens, 24 inches, alurninized Cer-Vit primary mirror of focal ratio $f/3$, and secondary mirror of 7 inches diameter, giving a Cassegrain focal ratio $f/13.5$. The Cassegrain focal plane is located 12 inches behind the primary mirror cell and the focalization is adjustable by electric drive mouvement ofthe secondary mirror.

The right-ascension and declination drives are exclusively motor driven. In both drives a three velocities system is available: a slow motor gives a drive rate of 3 degrees per time second; a servo amplifier-motor gives a set drive rate of 3 arc minutes per time second and a guide drive rate of 3 arc seconds per time second.

The selection of the desired rate in right-ascension or/and declination is made by the observer through a remote control paddle. Both right-ascension and declination drives can be pivoted slightly to provide backlash to allow balance adjustement.

An independent synchronous tracking motor gives the diurnal rate through a 30 inches diameter, preloaded tracking drive gear, attached to the polar axle shaft.

The telescope is provided with protections against dangerous positions near the horizon, excessive twisting of the interconnecting cables and mouvements with the drives in the balancing position, while the gears are partia1ly disengaged.

Perhaps the more interesting feature of the telescope is their special position digital read-outs. The telescope is provided with standard illuminated clock-type dials, indicating right-ascension to 10 second of time, hour angle to 1 minute of time and declination to 2 arc minutes. It is also provided with a remote console digital read-out, giving right-ascension and hour angle to 1 second of time and declination to 1/10 arc minute. This device is accurate enough to use the telescope in mapping survey over regions with dimensions of the order of one degree, as an actual off-set guider.

The telescope and their peripheric equipment are feeded from as electronic, voltage regulated power supply with integral protections against overloads. The tracking drive can alternatively be connected to the power line or to a locally made constant frequency power source.

Spectrograph

In spectroscopic works, the telescope operates with a matched Boller & Chivens model 26767 Cassegrain spectrograph illustrated in Fig. 1 and outlined in Fig. 2. This spectrograph has an off-axis parabolic, 50 mm working diameter, 675 mm focal length collimator, with screw adjustement and dial read-out of focus position; grating of 1200 grooves/mm blazed for 5000 Å in the first order (Litrov mode), with 64x64 mm ruled area; concentric Cassegrain-Maksutov camera with $f/3$ focal ratio, 6 inches focal length. It is provided with an adjustable slit and decker assembly allowing slit widths of 28,56,80,112 and 160 µm and slit lengths of 0.25, 2.5, 10 and 25 mm. The slit viewer consists of a rotating 10 x eyepiece with 1 inch diameter field at the slit.

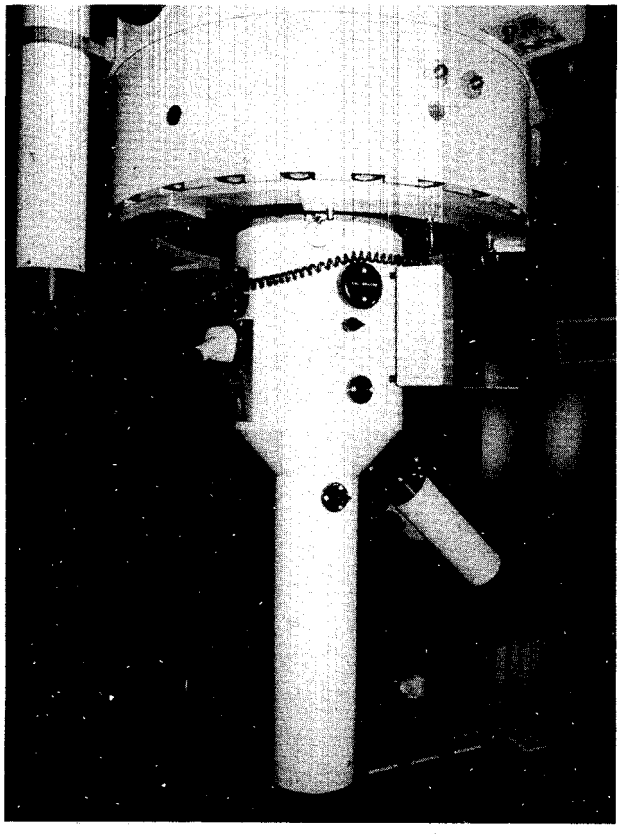

Fig. 1 - The picture shows the spectrograph mounted on the telescope; over the tabie, the OMA console, X-Y scope display and digital recorder.

The spectrograph is also provided with a filter holder ableto support filters of 1/4 x 1/4 inch and a shutter operated through an external control knob; a propactor with vernier and lock, indicating the grating angle, ti; a calibration source assembly consisting of an incandecent bulb feeded by a controlled voltage power supply, diffusers and condensing lens to give uniformity of illumination on the slit; and a comparison source assembly, consisting of an Helium-Argon lamp with power supply, to allow the measure of the wavelength corresponding toeach channel of the measured spectrum.

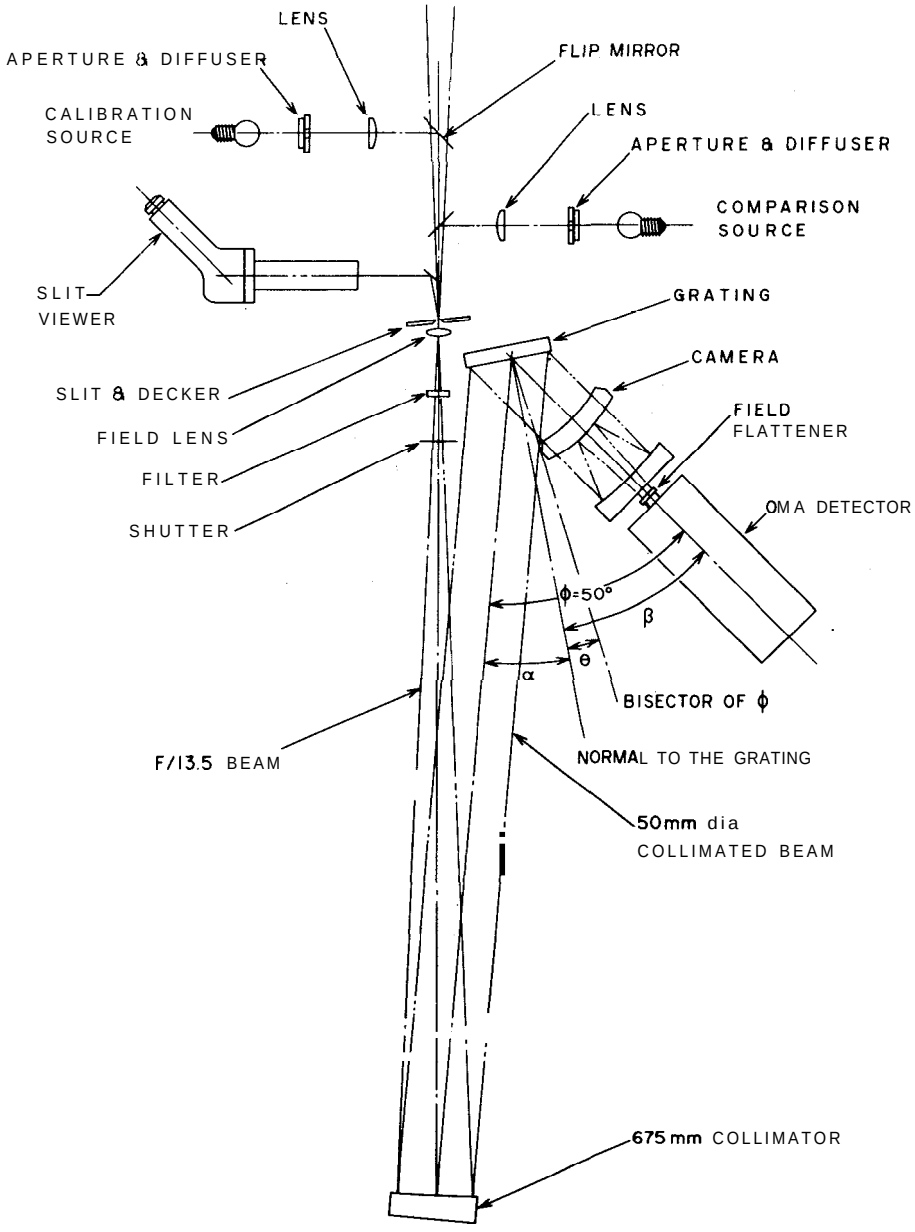

Fig. 2 - Optical diagram of the spectrograph showing the grating angles used in the text.

Optical Multichannel Analyzer

The output of the spectrograph feeds an optical multichannel analyzer (OMA), series 1200, manufactured by Princeton Applied Research Coorp. through a Silicon Intensified Target Oetector (SIT), model 1205--D.

The SIT consist of a silicon intensified target camera tube, deflection components, high voltage power supply, and preamplifier. The detector head has a two 0.2x0.5 inches input pattern, corresponding to 500 digitalized channel of the OMA, in two lines of detectionwindowsas shown in Fig. 3. The window width per channel at the detection inputis, therefore:

$$\omega = 0.5/500 \quad \text{inches} = 25.4 \ \mu\text{m} \tag{1}$$

The reciprocal linear dispersion, in Å/channel, wlll be equal to

$$\gamma_c = \omega\gamma = 0.0254 \ d\lambda/d\ell \tag{2}$$

where $\gamma = d\lambda/d\ell$ is the reciprocal linear dispersion at the outputofthe spectrograph, given in (12).

γ is a function of the grating angle, θ, but in all cases, the average reciprocal dispersion at the output of the OMA is of the order of 1 Å/channel; i.e., an average spectral range of 500 Å for each exposure cycle.

The spectrograph slit and decker assembly allows to use alternatively one or two simultaneous slits (except for the maximum height, h = 25 mm). When a slngle slit is being used it is found on the right side of the slit viewer field and its monochromatic projected areafalls on the first line of windows of the detector input pattern (see Fig.3). If a double slit is used, the slit centers are separated by 1.25 mm, which corresponds to a projected distance equal to 2.82 mm at the detector input. The right side slit will be centrally projected over the first line of detector input windows; and the left side slit will be projected over the second line of windows (also called dark line), as shown

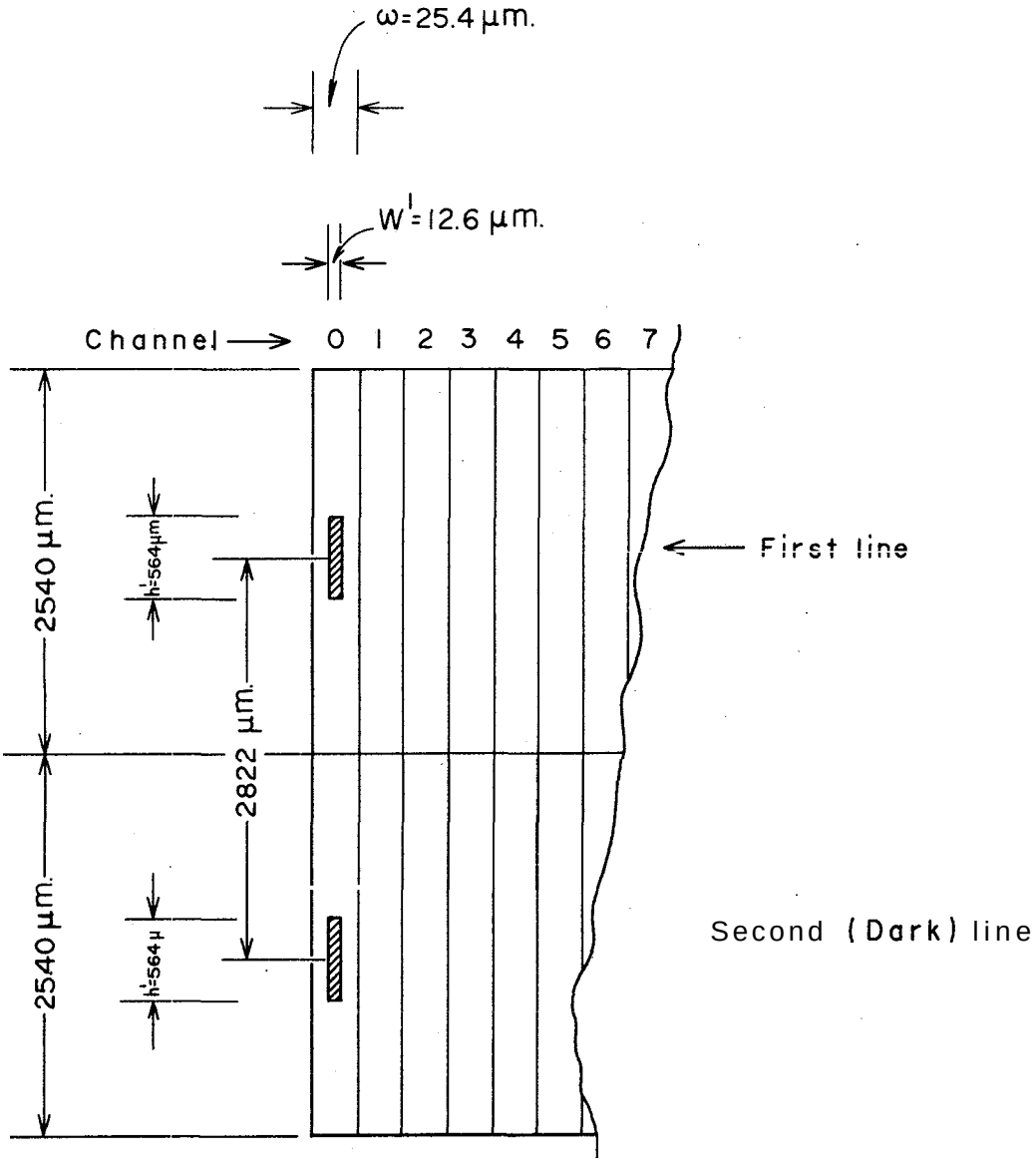

Fig. 3 - SIT detector input pattern, showing dimensions and monochromatic projected areas for a double slit with ω = 56μm and h = 2.5 mm.

in Fig. 3. This second line of detection windows allows an operating mode of the OMA, in which the counting of the charge contents of the dark line are automatically, channel-by-channel subtracted from the contents of the first line, eliminating from the memory accumulation the dark current and stray light contributions. This operating mode, associated

with the double slit feature of the spectrograph, permits to obtain stellar spectra by two measures, with the stellar image sucessivelyover the right and left side lifts. This is not the method generally used at Valinhos Station.

The response of the 1205-D detector is shown in Fig.4. It is over 10^{-2} count/phot. from 3600 Å to 7000 Å, with a maximum at 4300 Å.

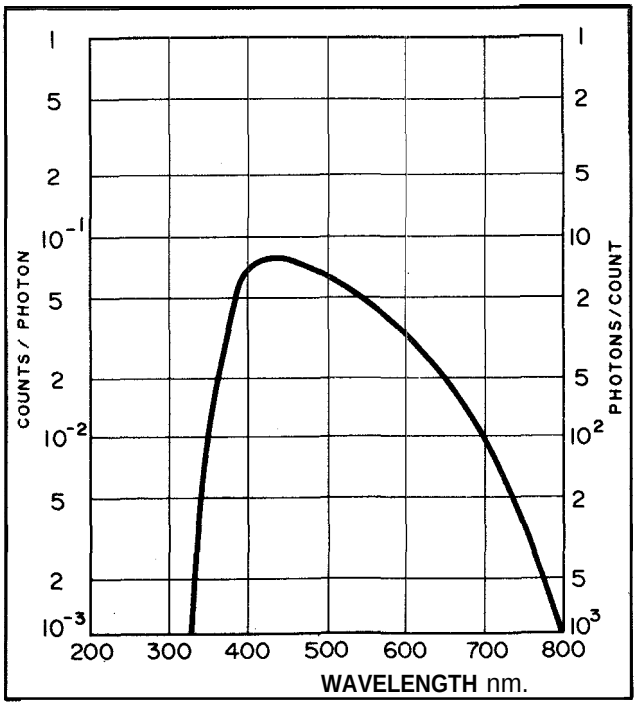

Fig. 4 - Response versus wavelength for the S-20, 1205-D SIT detector with model 1205 OMA.

The output of the detector is read one channel at a time by a scanning electron beam. The detector housing also contains the low-noise, controlled bandwidth prearnplifier. The high level signal from the preamplifier is routed to the 1205 OMA Console for further processing.

The OMA console has several functions. The first of these is to digitize the signal from the detector. Once in digital form, the data may be directed to either of two 500 word, 21-bit memories (Mem. A and Mem. B) These memories may be used to store the result of a single

2.8 ms (one frame) exposure or to signal-average many exposures, thus improving both the signal-to-noise ratio and the dynamic range. Generally the A memory is used to store the desired signal plus undesired signals (such as background sky light and detector dark current) and the B memory is used to store the undesired signals alone. The two memories may then be subtracted channel-by-channel to yield the desired signal. Once the data is in this form, each channel may be read digitally on the front panel or may be directed to an HP 5055 digital printer. A high-speed analog output is used to drive a model 604 Tektronix X-Y display scope and a slow analog output is being used to drive an HP paper recorder.

The OMA can be used in several operating modes:

Input Modes - In every input mode, the data from all five hundred detector channels is read into a memory. The data may be added to the A memory (A-Accum. button), to the B memory (B-Accum. button), or to both for any number of scans. It is also possible to select a delay of from zero-to-eleven times 32.8 ms between active read-in cycles. This allows the signal to accumulate on the detector before being applied to the preamplifier, thus improving the signal-to-noise ratio for weak signals. In addition, there is a test mode which provides a test input level with an artificial peak after the cursor channel.

Accumulation may be automatically stopped in two ways. Selecting the *Full Scale Hold* mode, the accumulation is stopped when the count in any channel reaches or exceeds 98.000. Selecting the Preset *Hold* mode, the accumulation is stopped after a preset number of read-in cycles. The accumulation time will be the number set on the Preset switch times the Delay switch plus one, times 32.8 ms. The measurement may be manually stopped at any time by releasing the respective Accum. button.

Display Modes - The output of either A or B memories, the channel-by-channel difference (A-B), or the Real Time (single frame scans of the Vidicon) are displayed on the Tektronix X-7 display scope. The OMA console has two controls to select the vertical sensitivity for the scope: the Scale Factor switch selects the magnitude of the most significant digit read from the memory to the display D-A converter; the Vertical Expand control varies the vertical gain from X1 to X10. There is also a

logaritmic display mode in which the log. of the selected data source is displayed.

An intensified channel on the display marks the location of the cursor, The cursor channel number is read out digitally on the OMA front panel, together with the contents of this channel. The cursor may be moved to the right or to the left or returned to channel zeroby pressing the respective buttons, thus allowing the reading of the channels of every channel.

The scope. display may be expanded in the horizontal direction by turning the Horizontal Expand control. In this mode, thedisplaystarts expanding at a point twelve channels to the left of the cursor.

There is also a summation mode in which the sum of the contents of any number of adjacent channels can be displayed in the OMA front panel. This is done by positioning the cursor on the leftmost channel to be summed and then pushing the Σ button. The cursor is then moved to the right until it is over the rightmost channel to be sumned. The sumnation will appear at the digital display. Moving the cursorfrom right-to left will subtract the contents of each channel from the summation. The displayed sum is multiplied by X10 or X100 as selected by a switch on the back panel and indicated by a LED to the rightofthefront panel display.

Principal Parameters

To estimate the more important parameters of the Spectrograph we will follow Schroeder[1], Bowen[2] and the Instruction Manual for the instrument.

Let us assume that a slit width, $\omega = 56$ μm and a slit height, $h = 0.25$ mm has been selected to some observation.

According to the above description, the diameter and focal length of the telescope are:

$$D = 24 \times 25.4 \text{ mm}; \qquad f = 13.5\, D$$

and similarly for the collimator

$$d_1 = 50 \text{ mm} \quad ; \quad f_1 = 675 \text{ mm}$$

and for the camera:

$$d_2 = 2 \times 25.4 \text{ mm} \; ; \quad f_2 = 6 \times 25.4 \text{ mm}$$

The grating constant is:

$$\tau = 1/12000 \text{ cm}$$

The angles subtended by the slit on the sky are:

$$\begin{aligned} \phi &= \omega/f = 6.8\times10^{-6} \text{ rad} = 1''.4 \\ \phi' &= h/f = 3.04\times10^{-5} \text{ rad} = 6''.3 \end{aligned} \tag{3}$$

and the angles subtended by the slit at the collimator are:

$$\begin{aligned} \Psi &= \omega/f_1 = 8.3\times10^{-5} \text{ rad} = 17''.1 \\ \Psi' &= h/f_1 = 3.76\times10^{-4} \text{ rad} = 1'17''.6 \end{aligned} \tag{4}$$

The projected slit width and height in the camera focal plane (without including the anamorphic effect of the grating) are:

$$\begin{aligned} \omega' &= \omega f_2/f_1 = 12.6 \text{ } \mu\text{m} \\ h' &= h f_2/f_1 = 56.4 \text{ } \mu\text{m} \end{aligned} \tag{5}$$

The angular dispersion of the grating can be obtained fromthe well-know relation:

$$\chi = \frac{\tau}{\kappa} (\text{sen } a + \text{sen } \beta) \tag{6}$$

where κ is the spectral order; λ, the wavelength; τ, the grating constant; a and β, the incident and refraction angles. This expression can easely be written in terms of the angles ϕ and θ of Fig. 2:

$$\lambda = \frac{2\tau}{\kappa} \cos\frac{\phi}{2} \text{ sen } \theta \tag{7}$$

At first order and being $\tau = 1/12000$ cm; $\phi = 50^0$, (7) becomes:

$$\lambda = 15100 \text{ sen } \theta \quad [\text{Å}] \tag{8}$$

which allows the selection of θ for the central wavelength to be observed.

For a fixed angle of incidence we can find the angular dispersion of the grating by differentiation of (6):

$$\frac{d\beta}{d\lambda} = \frac{K}{\tau \cos \beta} = \frac{\text{sen } a + \text{sen } \beta}{\lambda \cos \beta} \tag{9}$$

which, in terms of 8, ϕ, gives the reciprocal angular dispersion:

$$\frac{d\lambda}{d\beta} = \frac{\lambda}{2} (\text{cotg } \theta - \text{tg } \phi/2) \tag{10}$$

For our spectrograph, (10) becomes:

$$\frac{d\lambda}{d\beta} = \frac{\lambda}{2} (\text{cotg } \theta - 0.466) \tag{11}$$

The reciprocal linear dispersion at the output of the camera, in Å/mm will be:

$$\lambda = \frac{d\lambda}{da} = \frac{1}{f_1} \frac{d\lambda}{d\beta} = \frac{\lambda}{300} (\text{cotg } \theta - 0.466) \tag{12}$$

The corresponding reciprocal linear dispersion, in Å/chan. at the OMA output is indicated in Eq. (2).

Both y and $y_{c'}$ expressed by (12) and (2) are reciprocal linear dispersion for the central wavelength of the refracted spectrum. These values can be used through all the small spectral band, $\Delta\lambda$ - 500 Å, corresponding to one exposure cycle, with certain error. A more accurate computation is needed to obtain a better relation between wavelengths and channel numbers of the OMA detector, along the wavelength range of a single measurement.

Calling i the detector number ($0 \leq i \leq 499$), the distance from the channel i from the central one will be $(i - 249.5)\ \omega$, at the camera focal plane. The refraction angle, β_i, corresponding to the i channel, is (see Fig. 2 and 3):

$$\beta_i = \beta + \Delta\beta$$

where $\beta = \theta + \phi/2$ and $\Delta\beta$ - sen $\Delta\beta = (i - 249.5)\ \omega/f_2$.

This value of β_i, together with Eq. (9) give the reciprocal linear dispersion, in Å/mm, corresponding to the channel i:

$$\gamma_i = \gamma - \frac{\tau\omega(i - 249.5)}{\kappa f_2^2} \text{ sen } \beta \qquad (12.1)$$

where γ is given in (12)

According (2), the same reciprocal linear dispersion; in Å/ /channel, for the channel i, will be:

$$\gamma_{ci} = \gamma_c = \frac{\tau\omega^2(i - 249.5)}{\kappa f_2^2} \text{ sen } \beta \qquad (12.2)$$

For our spectrograph, in the first order (12.2) becomes:

$$\gamma_{ci} = \gamma_c - 2.3148\times10^{-4}\ (i-249.5) \text{ sen } (\theta+25^0) \qquad (12.3)$$

This (12.3) gives the number of Å corresponding to the channel i. Generally, the observer likes to know the wavelength range corresponding to a given pair of channels, say $i_1 = m$, $i_2 = n$ $(m < n)$. The desired wavelength range will be:

$$\Delta\lambda_{m,n} = \sum_{i=m}^{n} \gamma_{ci}$$

or:

$$\Delta\lambda_{m,n} = (n-m)\left[1.3889 \cos(\theta+25^0) - 1.1574\times10^{-4}(499-n-m)\,\text{sen}(\theta+25^0)\right] \qquad (12.4)$$

which provides a way to compute the wavelength for a given channel number, when the wavelength centered on another channel is know, from a comparison spectrum.

The important parameters of any spectrograph, determining the suitability of the instrument for a given observational program, are:

anamorphic magnification of the grating, n; spectral purity; $\delta\lambda$; spectral resolution R_e; efficiency, τ; throughput, L_e (sometimes called *luminosité*); throughput-resolution product, $L_e.R_e$; and spectrographic speed, s.

The anamorphic magnification is defined by:

$$r = \cos a / \cos \beta \tag{13}$$

which, in terms of θ, ϕ, becomes:

$$r = \frac{1+\text{tg}\,\frac{\phi}{2}\,\text{tg}\theta}{1-\text{tg}\,\frac{\phi}{2}\,\text{tg}\theta} = \frac{1+0.466\,\text{tg}\theta}{1-0.466\,\text{tg}\theta} \tag{14}$$

The effects of this factor r are as follows: the ratioof the dispersed beam width to the incident beam at the grating is $1/r$; the projected slit width in the camera focal plane is actually $\omega' = r\omega f_2/f_1$; the angle subtended by the projected slit width, ω', at the camera is $r.\Psi$. The name of anamorphic magnification is applied because r affects the beam and projected slit widths, but not the heights. It can beshown that when $r \neq 1$ other parameters are modified: the spectral purity is directly proportional to r; and the spectral resolution and the spectrographic speed are both inversely proportional to r.

To define the spectral purity it can be assumed that the entrance slit is illuminated by two monochromatic wavelengths separated by AA. The two images in the camera focal plane will be just separated when the angle between corresponding sides of the images is slightly greater than Ψ. When the images are in the verge of being resolved, AA $= \delta\lambda$, the last being called spectral purity. In that case, the condition

$$\delta\lambda = \Psi \,/\, \frac{d\beta}{d\lambda}$$

together with (3), (4) and the matching condition, $D/f = d_1/f_1$, gives:

$$\delta\lambda = \frac{\omega}{f_1}\,\frac{d\lambda}{d\beta} = \frac{\psi D}{d_1}\,\frac{d\lambda}{d\beta} \tag{15}$$

which, for our spectrograph, becomes:

$$\delta\lambda = 4.145\times10^{-5}\ \lambda(\text{cotg}\ \theta - 0.4666) \qquad (16)$$

By definition, the spectral resolution is:

$$R_e = \lambda/\delta\lambda = \frac{d_1\lambda}{D\psi}\ \frac{d\beta}{d\lambda} \qquad (17)$$

or:

$$R_e = 2.41\times10^4\ /\text{cotg}\ \theta - 0.466) \qquad (18)$$

The efficiency, r, of the spectrograph can be expressed as the product of bare aluminum film coated collimator mirror, camera, and grating efficiencies. Assuming the two firsts factors are 0.85, the spectrograph efficiency is:

$$\begin{aligned} \tau = 0.52 \ &\text{at}\ 4000\ \text{Å} \\ 0.59 \ &\text{at}\ 5000\ \text{Å} \\ 0.71 \ &\text{at}\ 5600 \end{aligned} \qquad (19)$$

The throughput, L_e, is related to the amountoflight transmitted by the telescope-spectrograph combination. It was shown by Jacquinot[3] that the flux transmitted, F, by any optical system is the product of the luminance, L, at the entrance apertura and the throughput of the system.

Considering only the spectrograph, the luminance is the intensity per unit area at the entrance slit. The throughput, as defined by Jacquinot is the product of the solid angle of the entrance slit subtended at the collimator, the collimator area, and the spectrograph transmittance, τ. It is found that:

$$L_e = \pi\tau d_1^2\ \Psi\ \Psi'/4 = \pi\tau D^2\ \psi\ \psi'/4 = \pi\tau D^2\omega h/4f^2 \qquad (20)$$

which, for our spectrograph, becomes:

$$L_e = 143\ \tau\ \omega\ h \qquad (21)$$

An important measure of the merit .of a given spectrograph is the througtiput-resolution product, which is:

$$L_e, R_e = \frac{\pi \tau d_1 D \psi' \lambda}{4} \frac{d\beta}{d\lambda} \qquad (22)$$

or, in terms of 8 and for the selected values of ω, h:

$$L_e \cdot R_e = 1.45 \times 10^6 \tau / (\coth \theta - 0.4666)\,\mu m^2 \qquad (23)$$

The relation (22) is most useful when comparing different spectrographs for use on the same telescope under similar conditions of seeing. When considering different seeing conditions, or extended sources, it is also necessary to take into account the luminanceofthe source at the spectrograph entrance slit. From the definition of luminance (see p.e. Longhurst[4], for a complete discussion on photometric parameters) it can be see that for a point source $L\alpha(\psi')^{-2}$, while for an extended source of uniform surface brightness, L = constant, whenthe source's angular diameter is large compared to the seeing limit. If these results are incorporated into (22), the following expression for the transmitted flux-resolution is found:

$$F \cdot R_e \alpha \begin{cases} \dfrac{\tau d_1 DA}{\psi'} \dfrac{d\beta}{d\lambda} & \text{for point sources} \qquad (24) \\ \tau d_1 D \lambda \psi' \dfrac{d\beta}{d\lambda} & \text{for extended sources} \qquad (25) \end{cases}$$

From (24), it can be seen that better seeing (smaller ψ') results in a larger transmitted flux-resolution product, as expected. If the seeing disk is larger than the angular width of the entrance slit ($\psi' > \psi$), then increased resolution can be obtained only at the expense of transmitted flux. In Eq. (25), the factor ψ' is not related to the seeing; it is simply the angular height of the entrance slit projected on the sky.

The spectrographic speed is proportional to the flux per unit area that the spectrograph yields at the detector input. According Bowen[2], the width of this area can be taken as the distance which covers a wavelength range of 1 Å. If the reciproca1 linear dispersion is y, in units of Å/mm, then this distance is simply $1/\gamma$ mm. For an effec-

tive entrance slit height h (which may be the diameter of a seeing-broadened point source) the height of the area on the detector is h'. The detector are is then h'/γ.

From (18), (24) and (25), the following expressions for the transmitted flux are obtained:

$$F\alpha \begin{cases} \tau D^2 \psi/\psi' & \text{for point sources} \quad (26) \\ \tau D^2 \psi\psi & \text{for extended sources} \quad (27) \end{cases}$$

Denoting the speed by S it is found, for a seeing broadened point source, that:

$$S \text{ a } \tau D^2 \gamma\psi/\psi' h' \quad (28)$$

and

$$S \alpha \tau\ D^2 \gamma\ \psi\psi'/h' \quad (29)$$

for extended sources.

Two cases can be considered, following Bowen[2]: Case A - All the light passes the entrance slit, in which case $\psi = \psi'$, h' = ω' and:

$$S \alpha \tau\ D^2 \gamma\ \omega' \quad (30)$$

For photographic detectors ω' is normally taken as the limit of resolution of the emulsion. For our OMA detector such a limit can be taken as the distance between centers of two adjacent channels (1):

$$\omega' = \omega = 25.4\ \mu m.$$

Case B - The entrance slit is narrower than the image ($\psi' > \psi$), in which case:

$$S\ a\ \frac{\tau\ \omega' \gamma^3 d^2}{(\psi^1)^2 1} \left[\frac{d\beta}{d\lambda}\right]^2 \quad (31)$$

For exterided sources, it is obtained:

$$S \alpha \tau\ \omega' \gamma^3\ d_1^2 \left[\frac{d\beta}{d\lambda}\right]^2 \quad (32)$$

The selection of the slit dimensions to be used in the observation of a given source can be made from the above expressions, taken into account the source type and the seeing conditions during the rneasurernent.

Exemple of Observation

For the purpose of illustration, let us assume that a 5th magnitude star spectrum is to be measured in a limited ban around 4400 Å.

For such stellar source, assuming good seeing conditions, it can be selected ω = 28 μm and h = 0.25 mm.

The angle of the grating, θ, is related to the central wavelength by Eq. (8). For 17^0, it is obtained λ_c = 4415 Å. The central reciproca1 linear dispersion, given by Eq. (2), is γ_c = 1,048 Å/channel. The 500 channels of the detector will cover in this case a spectralband of about 524 Å, centered on 4415 Å. The actual wavelength corresponding to each channel can be determined recording a comparison spectrum from the A-He lamp source, after or before the stellar measurement, with the same grating setting. It is a good practice to take the comparison spectrum in the same telescope position of the stellar observation, toavoid eventual shifting due to flexures.

The collimator must be focussed at this stage, accordingthe selected grating angle. The empirical relation between θ and the collimator focal dial read-out, E, is

$$\varepsilon = 0.0023\ \lambda_c - 7.1 \qquad (33)$$

which, in our case, gives: E = 3.05.

The integration time, T, must be now selected. As it was explained above, T is given by:

$$T = 32.8\ (D+1)P \quad \text{ms} \qquad (34)$$

where D is the delay, or the number of signal-average 32.8 ms exposures, over the first, composing one read-in cycle; and P is the preset number of read-in cycles.

Our uncooled 1205-D detector admits a maximum delay $D = 3$. This allows four accumulations cycles for each read-in cycle, which is the delay normally used at the Valinhos Station. The number of active read-in cycles, P, must be selected taking into account that iricreasing P a better spectrum will be obtained, but the maximum count inany channel must not exceed 98000. For a 5th magnitude star in normal conditions a good measure is obtained with $P = 300$; i.e., T - 40 sec. Both D and P are fixed through the respective thumbwheel switch at the CMA front panel.

Once the star image is centered over the slit, the measurement can be initiated. For that, the A-Mem. display, A-Mem. erase, Preset-Hold and A. Accum. buttons must be pressed in order.

At the end of the selected integration time, the counting is automatically stopped and the Preset-Hold lamp lights up. The contents of all the 500 channel are shown in the X-Y scope display. Also each content can be digitally read on the CMA front panel, together with the channel nurnber, the changing of channel being made through the → or ← buttons.

As it was explained above, the contents of the A memory at this stage correspond to the net stellar flux plus the sky background, stray light and detector dark current. To isolate the net stellar flux a second measure must be made. By a small mouvement of the telescopethe star image is removed from the slit and a new counting can be directed to the B memory (pressing nor the B-Accum. button instead of the A-Accum. button in the sequence above). When this second counting cycle is finished, the net stellar flux in each channel can be read on the CMA front panel by pressing the A-B button. The X-Y scope will then display the desired net spectrum. The contents of all the 500 channels can be paper impressed by the HP digital recorder, by pressing the Plot/Print button. The count in each channel is identified by the respective channel number in the record.

To look the main features of the measured spectrum it is sometimes useful to take a photograph of the scope display with a Polaroid camera or a paper record of the spectrum through the rear slowanalogic output with the HP milivoltmeter, also available at the Station.

Of course, if a wider range of the source spectrum is desired, it is necessary to repeat the described procedure forother grating settings.

A method for data reduction is given in Apendix 1, which allows to eliminate the effects of atmospheric selective absorption, applying to diffuse sources. A similar analysis can be used for stellar spectra.

3. THE PLANETARY NEBULAE NGC 6818 AND NGC 7009

NGC 6818

NGC 6818 is a southern planetary nebula whose coordinates (1950) are: $a = 19^h41^m06^s$ and $\delta = -14^0 16'$. Its radius is about 9.1 arc seconds. The observations of this object were made on the nights of 8/9 and 9/10 September 1977 with reasonable sky conditions. As a comparison star, was choosen HR 7379, an AO spectral type. The spectrograph slit was aligned on the North-South direction and we have used a slit-width of 4'', placed along the region of higher brightness. The integration time, including background accumulation, was 3^m44^s for each spectral band of 500 Angstrons of the nebula and 3^m05^s for the comparison star. Thus, an all set of observations is done in about 35^m.

NGC 7009

This is alsoa southern nebula with coordinates (1950): $a = 21^h01^m30^s$ and $\delta = -11^0 34'$. The radius of this nebula is about 13.4 arc seconds. This planetary nebula is interesting because it shows a double ring structure and striking ansae. A detailed study of this object was presented by Aller and Epps. The observations were done on the same nights as NGC 6818 and HD 200761, an AO star, was choosen as a comparison. The other conditions were similar to those described before. In this case, the slit was placed along the bright ring in the NS direction.

Table 1 shows the observed intensity of the identified lines as well as the corrected intensity through the interstellar reddening. The data reduction method is given in the appendix 1.

Table 1

Element/line	NGC 6818		NGC 7009	
	I_0	I_c	I_0	I_c
[O II] 3727	65.3	73.9	7.0	7.9
[Ne III] 3869	55.9	62.2	86.9	96.1
Hγ 4340	41.6	44.0	42.7	45.0
[O III] 4363	11.2	11.8	4.5	4.7
He I 4471	-	-	1.3	1.4
He II 4686	34.3	35.0	14.5	14.7
Hβ 4861	100.0	100.0	100.0	100.0
[O III] 4959	373.2	369.9	261.6	259.4
[O III] 5007	1224.0	1208.0	868.9	858.2
He I 5876	-	-	11.7	10.6
Hα 6563	281.0	245.0	-	-
[N II] 6584	28.0	24.4	6.7	5.9

I_c ≡ Reddening corrected intensity

I_0 ≡ Observed intensity

The electron temperature of the nebulae can be estimated from the ratio of the nebular and auroral (forbidden) lines of O III (see appendix 2). The results that we have obtained are given in table 2 compared also with previous estimates.

The electron density could be, in principle, estimated from the 3726/3729 doublet line ratio of O II. However the sky conditions during our observations were not good enough to resolve the doublet and only the total intensity could be obtained.

Table 2

Object	Electron Temperature	Author
NGC 6818	11000 ^{0}K	Present
	11700 ^{0}K	Aller & Epps[5]
NGC 7009	9430 ^{0}K	Present
	10300 ^{0}K	Aller & Epps[5]

Once the electron temperature is determined, the ionic densities can be estimated from the line intensities. The basic equations and the prescriptions to correct for other ionization stages are given in the appendix 2.

Table 3 showsthe resulted elemental abundance ratios. We give also the results for the bright ring of NGC 7009, following the work of Aller & Epps[5]. The He abundance is quite good since doesn't depend strongly on the electron temperature. The other ratios are more sensitive to this parameter and therefore the uncertainties are greater. Nevertheless our results and those of Aller & Epps agree within a factor three for Ne and N and are in very good agreement for He and O.

Table 3

Object	He/H	O/H	N/H	Ne/H	Author
NGC 6818			9.3×10^{-5}	1.9×10^{-5}	Present
NGC 7009	0.12	3.8×10^{-4}	9.5×10^{-5}	3.8×10^{-5}	Present
	0.12	3.7×10^{-4}	3.3×10^{-5}	1.0×10^{-4}	Aller & Epps[5]

4. THE LAGOON NEBULA

The H II region, the Lagoon Nebula (M8; NGC 6523), is a southern object ($\alpha_{50} = 18^h01^m$; $\delta = -24^0$) with a diameter of about 25 arc minutes and a total ionized gas mass of the order of $10^3\ M_\odot$.

This nebula was observed on two consecutive nights (11/12 and 12/13 September 1977) in three different positions with the objective to measure possible temperatures gradients. However, the observations were done in the west part of the sky, where the lights from Campinas affect the measurements and due to the epoch, the observations were also done at considerable zenithal distances. Therefore, the present observations are of poor quality and we report only the results for the brightest measured point. We plan to observe this nebula in the next season with more favourable conditions.

In the position two, placed at about 60 arc seconds west from 9 Sgr, the brightest point we have measured, it was possible to estimate the relative intensity of the doublet 3729/3726 of O II and therefore to estimate the electron density. We have obtained $I(3729)/I(3726) = 0.82$, which corresponds to an electron density of $1.3\times10^3\ cm^{-3}$, typical for such a nebula. The electron temperature, obtained from the nebular and auroral lines of O III was 10240 ^{0}K.

Table 4 shows the observed intensities of some common lines also measured by Peimbert and Costero[6] in a nearby region. The agreement

Table 4

Element/line	Present	Peimbert & Costero[6]
[O II] 3727	126.6	126.0
O III] 4959	84.7	79.5
[O III] 5007	212.4	417.0
He I 5876	32.1	13.8
Hα 6563	507.1	407.0
[N II] 6584	28.8	83.1

Remark: $I_{H\beta} = 100$

is good for some Oxygen lines but is poor for the red lines, specially for the λ6584 [N II] line. We remark that the theoretical value for the ratio $I(5007/I(4959)$ of OIII is 3.0, while Peimbert and Costero have obtained a ratio of about 5.2 and we have obtained 2.5, in better agreement with the expected value. This by no means says that our observations are the best, but that more careful measurements should be done.

5. THE ORION NEBULA

This nebula around the star θ^2 Ori has been the mostobserved H II region of the sky due to its large angular size (several arc minutes), low reddening and very high emission. It can be observed from both the southern and northern hemisphere (approximate central coordinates $\alpha \sim 5^h34^m$, $\delta \sim -5^0 25'$) providing a comparison source for photometric and spectroscopic studies of other nebular regions. It is impossible to give a complete bibliography concerning this object; but, between the more relevant and recent spectroscopic works, it can be mentioned: Cruvellier[7]; Robbins[8]; Caplan[9]; Simpson[10]; Fehrenbach[11]; Peimbert and Torres-Peimbert[12].

We observed the Orion Nebula on the nights 9/10, 11/12 and 12/13 September 1977. Four non central points were selected for measuring, shown in Fig. 5. These observations were made with a medium-poor sky quality and results are reported only to illustrate the instrument performance. (More recents measuring, still not reduced, show that results are very sensitive of the sky seeing conditions). A delay D = 3 preset Ps = 800 were used, giving an integration time of 105 sec. for each measure. The slit dimensions were ω = 160 μm and h = 2.5 mm.

Table 5 shows the reduced relative intensities of the detected lines.

The ratio $I(3729)/3726)$ was computed by graphical restitution of the line shapes from the histograms in the respective spectral range, for each observed point. These ratios of the [O II] doublet allow the evaluation of the electron densities (Appendix 2), which are show

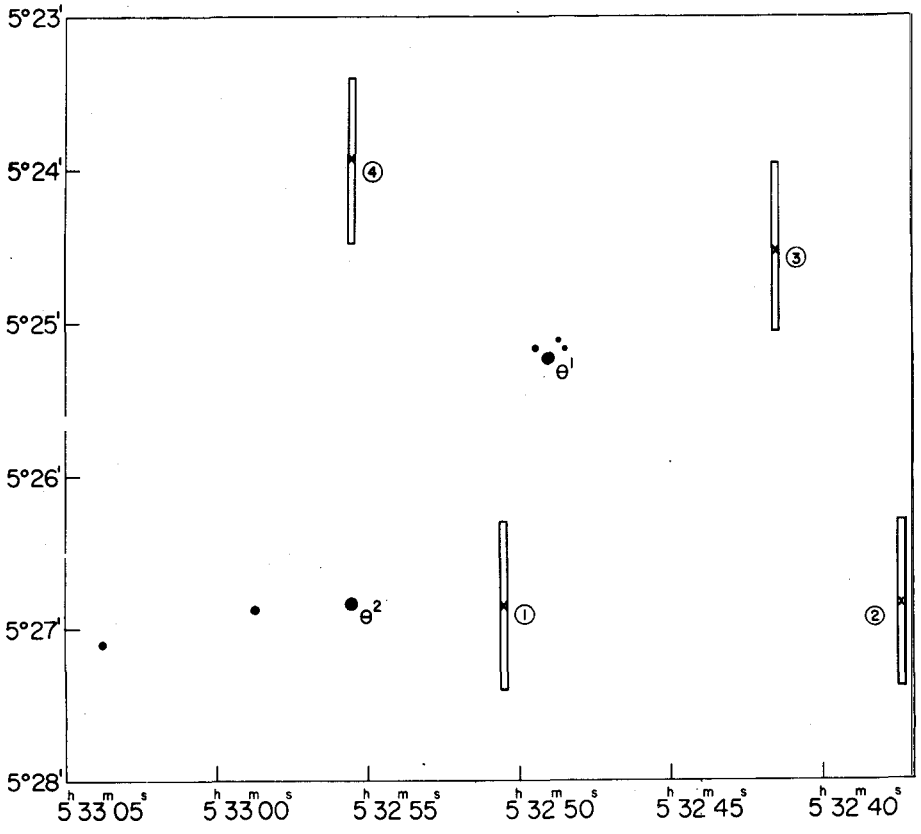

Fig. 5 - Sky Projections of the slit (1, 2, 3 and 4) for the observed regions of the Orion Nebula. Coordinates are of epoch 1950.

in Table 6. Our results are consistent with the ones obtained in recent researches (Elliot & Meaburn[13]; Caplan[9]) but somewhat hight in relation to Caplan measurements, for points coincidents with central position of our slit. These differences can be due to our low angular resolutions; each position of our slit covers a long strip of the nebula and so our results correspond to severa1 regions measured by Caplan.

The electron temperature was evaluated through the ratio of nebular and aurora1 lines of [O III] : $I(4959 + 5007)/I(4363)$. The low level of emission at $\lambda 4363$ over the noise prevent quantitative results for all but the point 1.

Applying formula of Appendix 2 and using values of T_e given by other workers for regions 2, 3 and 4, some abundances were computed, which are shown in Table 6. The values obtained are in accordance with the ones resulting from more detailed studies referred in the literatu-

re (Peimbert and Torres-Peimbert[12]) for respectives regions of the nebula.

These preliminary results, although obtained in nights ofnot very good seeing conditions, allow us to say that the instrurnent is sui-

Table 5

Elem./lines \ Reg.		100 $IP/I(H_\beta)$			
		1	2	3	4
[O II]	3726	109.4	129.7	86.8	65.3
[O II]	3729	53.4	80.9	58.7	43.7
H_κ	3750	15.4	-	-	-
H_θ	3798	10.1	-	-	-
[Ne III]	3869	9.4	-	-	-
H_ζ	3889	15.5	-	21.1	-
H_εN III	3970	24.9	-	21.9	-
$H\gamma$	4340	47.5	37.6	*	-
[O III]	4363	0.6	-	*	-
He I	4471	4.0	2.1	*	-
[O III]	4959	63.9	65.2	61.9	46.9
[O III]	5007	210.9	204.7	200.5	168.1
N II	6549	30.6	-	12.8	13.7
tia	6563	836.8	523.4	309.1	351.0
[N II]	6583	99.1	37.4	44.6	36.1
He I	6678	6.1	-	-	-
[S II]	6717	11.2	-	4.0	

* The lack of data at these wavelengths is due to limitations of observing time; this range was not measured for points 3 and 4.

table for measuring physical parameters of typical high and medium level emission H II regions and planetary nebulae.

Table 6

	Region			
	1	2	3	4
N_e	6300	2700	2100	2200
T_e	7900	-	-	-
He/H	0.08	-	-	-
O/H	3.1×10^{-4}	3.1×10^{-4}	3.1×10^{-4}	2.4×10^{-4}
N/H	6.5×10^{-5}	2×10^{-5}	3.1×10^{-5}	2.6×10^{-5}
Ne/H	4.2×10^{-5}	-	1×10^{-5}	-

APPENDIX 1

The Data Reduction Method

The data analysis which is outlined below is to be mainly applied to emission lines from diffuse objects such as planetary nebulae and H III regions.

Let N_k the number of counts in channel k in a given integration time t_ℓ

The total number of counts in the line will be

$$N_\ell = \int_{\text{line}} S_k(N_k - N_c)dk = \sum_k S_k(N_k - N_c) \qquad A(1)$$

where N_c is the number of counts per channel of the neighbouring continuum, and S_k is the detector sensibility at the k-channel.

The energy intensity of the line will be

$$I_\ell = \alpha \frac{N_\ell}{t_\ell} e^{\tau_\ell} = \alpha \frac{\sum_k (N_k - N_c) S_k}{t_\ell} e^{\tau_\ell} \qquad \text{A(2)}$$

where α is an average scale factor (in erg cm^{-2} $count^{-1}$ if I_ℓ is given in erg cm^{-2} s^{-1}) characteristic of the detector and the exponential factor takes into account the atmospheric extinction.

If we are interested only in relative intensities, we observe a comparison star for which we know the relative spectral intensity. If we choose a nearky star in order that the air masses (object and comparison star) are practically the same during the observations, the intensity of the star near the spectral region of the line under considerations is:

$$I_{*,\ell} = \alpha \frac{\langle N_k^* S_k \rangle_\ell}{t_{*,\ell}} \frac{\lambda^2_\ell}{D_\ell C} e^{\tau_\ell} \qquad \text{A(3)}$$

where $\langle N_k^* S_k \rangle_\ell$ is the average number of counts per channel centered on the line, obtained in a integration time $t_{*,\ell}$, λ_ℓ is the line wavelength, D_R is the dispersion of the spectrograph detector at the considered wavelength (in Angstron per channel) and C is the light velocity.

From eqs. A(2) and A(3) one obtains:

$$\frac{I_\ell}{I_{*,\ell}} = \frac{\sum_k (N_k - N_c) S_k}{\langle N_k^* S_k \rangle_\ell} \left(\frac{t_{*,\ell}}{t_\ell} \right) \frac{D_\ell C}{\lambda^2_\ell} \qquad \text{A(4)}$$

Considering the intensity of a given line ℓ with respect some reference line ℓ_0 ($H\beta$ in general) and that the detector sensibility doens't vary to much in the neighbouring channels, 'the eq. A(4) can be written in the form

$$\frac{I_\ell}{I_{\ell_0}} = \left(\frac{D_\ell}{D_{\ell_0}} \right) \left(\frac{\lambda_{\ell_0}}{\lambda_\ell} \right) \left(\frac{t_{*,\ell}}{t_{*,\ell_0}} \right) \left(\frac{t_{\ell_0}}{t_\ell} \right) \frac{\sum_k (N_k - N_c)}{\sum_{k_0} (N_{k_0} - N_{c_0})} \frac{\langle N_k^* \rangle_{\ell_0}}{\langle N_k^* \rangle_\ell} \left(\frac{I_{*,\ell}}{I_{*,\ell_0}} \right) \qquad \text{A(5)}$$

The equation A(5) is in the form actually used in the present work. The different integration times are fixed previously in the counter, the dispersion is obtained from the calibration spectrum, the different counts are obtained from the experimentand the relativestar spectra1 intensity is obtained from the litterature (see, for instance, O'Connell[14]).

Figure 6 shows the relative energy distribution for stars of spectral type in the range AO-A3 in the main sequence, taken from the work of O'Connell[14], which was used in the present analysis.

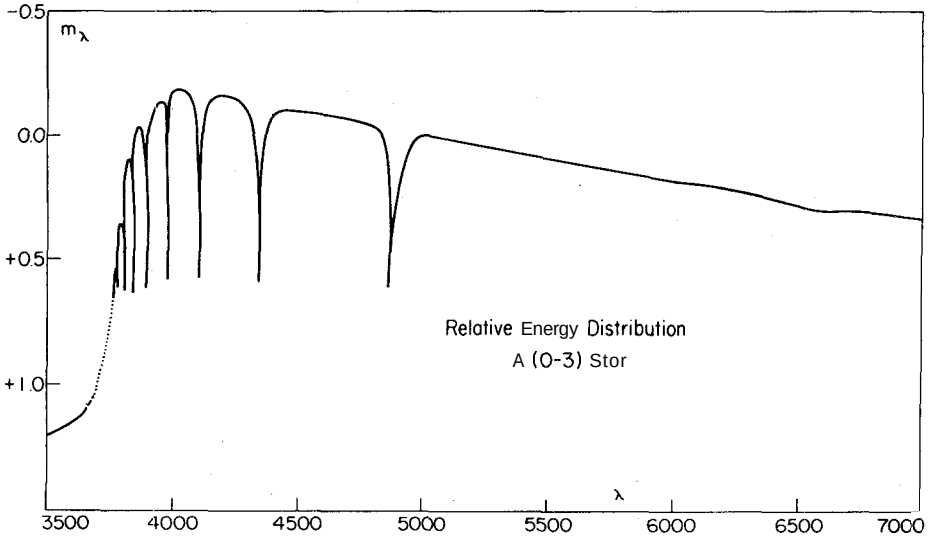

Fig. 6 - Relative energy distribution for stars of spectral type in the range AO-A3 in the main sequence taken from O'Connell[14].

APPENDIX 2

Evaluation of the Electron Temperature

For electron densities smaller than 10^5 cm^{-3}, the ratio of the nebular and aurora1 lines of O III and the ratio of the red and orange lines of N II depend practically on the electron temperature. Frorn the solution of the statistical equilibrium equations one obtains

$$\frac{I(4959 + 5007)}{I(4363)} = \frac{7.2}{(1 + 0.063x)} \exp\left[\frac{32970}{T_e}\right] \qquad A(6)$$

and

$$\frac{I(6548 + 6583)}{I(5755)} = \frac{7.53}{(1 + 0.27x)} \exp\left[\frac{25000}{T_e}\right] \qquad A(7)$$

where $x = \frac{10^{-2} n_e}{\sqrt{T}}$, as usual.

Helium Ionic Abundance

The He lines are essentially recombinations lines. Therefore from the knowledge of the effective recombination coefficients one obtains:

$$\left[\frac{He^{++}}{H^+}\right] = 0.0872 \left\{\frac{T_e}{10^4\ ^0K}\right\}^{0.111} \cdot \frac{I(\lambda 4686)}{I(H\beta)} \qquad A(8)$$

and

$$\left[\frac{He^{+}}{H^+}\right] = \begin{cases} 2.046 \left\{\frac{T_e}{10^4\ ^0K}\right\}^{0.123} \frac{I(\lambda 4471)}{I(H\beta)} \\ 0.988 \left\{\frac{T_e}{10^4\ ^0K}\right\}^{0.219} \frac{I(\lambda 5876)}{I(H\beta)} \end{cases} \qquad A(9)$$

Oxigen Ionic Abundance

From the solution of the statistical equilibrium equations one obtains

$$\left[\frac{O^+}{H^+}\right] = 8.20 \times 10^{-7} \left\{\frac{10^4\ ^0K}{T_e}\right\}^{0.424} \cdot \frac{I(\lambda 3727)}{I(H\beta)} \exp\left[\frac{38613}{T_e}\right] \qquad A(10)$$

and

$$\left[\frac{O^{++}}{H^{+}}\right] = 1.36\times10^{-6}\left(\frac{10^{4}\ ^{0}K}{T_e}\right)^{0.424} \cdot \frac{I(4959+5007)}{I(H\beta)} \exp\left[\frac{28880}{T_e}\right] \quad A(11)$$

The oxygen abundance, taking into account the other ionization stages, is estimated from the prescription

$$\left[\frac{O}{H}\right] \simeq \left[\frac{(He^{+}+He^{++})}{He^{+}}\right] \left[\frac{O^{+}+O^{++}}{H^{+}}\right] \quad A(12)$$

Nitrogen Ioniic Abundance

Analogous, for the nitrogen one obtains

$$\left[\frac{N^{+}}{H^{+}}\right] = 2.16\times10^{-6}\left(\frac{10^{4}\ ^{0}K}{T_e}\right)^{0.424} \cdot \frac{I(\lambda6584)}{I(H\beta)} \exp\left[\frac{21900}{T_e}\right] \quad A(13)$$

and the total abundance

$$\left[\frac{N}{H}\right] \simeq \left[\frac{O}{O^{+}}\right] \left[\frac{N^{+}}{H^{+}}\right] \quad A(14)$$

Neon Ionic Abundance

For the violet lines of Ne III, the statistical equations give us

$$\left[\frac{Ne^{++}}{H^{+}}\right] = 1.91\times10^{-6}\left(\frac{10^{4}\ ^{0}K}{T_e}\right)^{0.424} \cdot \frac{I(3869+3867)}{I(H\beta)} \exp\left[\frac{37186}{T_e}\right] \quad A(15)$$

and the total abundance

$$[a] \simeq \left[\frac{O}{O^{++}}\right]\left[\frac{Ne^{++}}{H^{+}}\right] \qquad A(16)$$

In order to obtain the numerical coefficients given in the equations above, we have used the effective recombination coefficients for He and H calculated by Brocklehurst[15,16]. For the N, O, Ne lines we have used the transition probabilities calculated by Seaton and Osterbrock[18] and Nussbaumer[19]. Collision strengths are those calculated by Seaton[17] and Pradhan[20].

Electron Densities

The ratio of line intensities of [O II], $I(3729)/I(3726)$, is rather independent of the temperature, and gives a measure of the electron density. Eissner *et al*[21] evaluate the relation between Ne and this ratio. For $\chi = 10^{-7}\ Ne/T^{1/2}$.

log χ	$I(\lambda3729)/I(\lambda3726)$		
	$T = 5\times10^3$	$T = 10^4$	$T = 1.5\times10^4$
-4.0	1.51	1.49	1.48
-3.5	1.51	1.49	1.48
-3.0	1.50	1.48	1.47
-2.5	1.47	1.45	1.44
-2.1	1.39	1.37	1.36
-1.5	1.19	1.17	1.15
-1.0	0.88	0.86	0.84
-0.5	0.59	0.58	0.57
0.0	0.44	0.43	0.43
+0.5	0.38	0.38	0.37
1.0	0.36	0.36	0.35
1.5	0.35	0.35	0.35
2.0	0.35	0.35	0.35

One of the authors (JAFP) thanks the financial support given by the Fundação de Amparo à Pesquisa do Estado de São Paulo (FAPESP) in the acquisition of such an equipment. This research was partially also supported by CNPq (SJCL).

REFERENCES

1. Schroeder, D.J. 1974 *Method of Experimental Physics* (Carleton N. ed.) Vol. 12, Chapt. 10, Academic Press NY.

2. Bowen, I.S. 1962, *Stars and Stellar Systems* (Kuiper G.P. and Middlehurst B.M. eds.) Vol.2, pg.34, Un Chicago Press.

3. Jacquinot, P. 1954. J. Opt. Soc. Amer. 44, 761.

4. Longhurst, R.S. 1967, *Geometrical and Physics Optics*, 2^{n} ed. Chapt. 18, Wiley, NY.

5. Aller, L. and Epps, H.W. 1975, Astrophys. J. *197*, 175.

6. Peimbert, M. and Costero, R. 1969, Bol.Obs.Ton.Tac. *5*, 3.

7. Cruvellier, P. 1967, Ann. d'Astrophys. 30, 1101.

8. Robbins, R.R. 1970, Astrophys. J. 160, 519.

9. Caplan, J.G. 1972, Astron. and Astrophys. *18*, 408.

10. Simpson, J.P. 1973, Publ.Astr.Soc.Pac. *85*, 479.

11. Fehrenbach, Ch. 1976, Astron. and Astrophys. Suppl. 29, 71.

12. Peimbert, M. and Torres-Peirnbert, S. 1977, Month.Not.Roy.Soc. *179*, 217.

13. Elliot, K.H. and Meaburn, J. 1973, Astron. and Astrophys. *27*, 367.

14. O'Connell, R.W. 1973, Astron. J. *78*, 1074.

15. Brocklehurst, M. 1971, Month.Not.Roy.Astron.Soc. *153*, 471.

16. Brocklehurst, M. 1972, Month.Not.Roy.Astron.Soc. *157*, 211.

17. Seaton, M.J. 1975, Month.Not.Roy.Astron.Soc. 170, 475.

18. Seaton, M.J. and Osterbrock, D. 1957, Astrophys. J. *125*, 66.

19. Nussbaumer, H. 1971, Astrophys. J. *166*, 411.

20. Pradhan, A.K. 1976, Month.Not. Roy. Astron. Soc. *177*, 31.

21. Eissner, W.; Martins, A.P.; Nussbaumer, H.; Saraph, H.E. and Seaton, M.F. 1969, Month.Not.Roy.Astron.Soc. 146, 63.